Anomalous spin waves and the commensurate-incommensurate magnetic phase transition in LiNiPO$_4$

T. B. S. Jensen,[1] N. B. Christensen,[1,2,3] M. Kenzelmann,[2,4] H. M. Rønnow,[2,5] C. Niedermayer,[2] N. H. Andersen,[1]
K. Lefmann,[1,3] M. Jiménez-Ruiz,[6] F. Demmel,[7] J. Li,[8] J. L. Zarestky,[8] and D. Vaknin[8]

[1]*Materials Research Division, Risø DTU, National Laboratory for Sustainable Energy, Technical University of Denmark,
DK-4000 Roskilde, Denmark*
[2]*Laboratory for Neutron Scattering, Paul Scherrer Institut and ETH Zürich, CH-5232 Villigen, Switzerland*
[3]*Nano Science Center, Niels Bohr Institute, University of Copenhagen, Universitetsparken 5, 2100 København Ø, Denmark*
[4]*Laboratory for Solid State Physics, ETH Zürich, CH-8093 Zürich, Switzerland*
[5]*Laboratory for Quantum Magnetism, École Polytechnique Fédérale de Lausanne (EPFL), 1015 Lausanne, Switzerland*
[6]*Institut Laue Langevin, BP 156, F-38042 Grenoble Cedex 9, France*
[7]*Rutherford Appleton Laboratory, ISIS Facility, Didcot OX11 0QX, Oxon, England*
[8]*Department of Physics and Astronomy and Ames Laboratory, Iowa State University, Ames, Iowa 50011, USA*
(Received 30 January 2009; published 20 March 2009)

Detailed spin-wave spectra of magnetoelectric LiNiPO$_4$ have been measured by neutron scattering at low temperatures in the commensurate (C) antiferromagnetic (AF) phase below $T_N=20.8$ K. An anomalous shallow minimum is observed at the modulation vector of the incommensurate (IC) AF phase appearing above T_N. A linear spin-wave model based on Heisenberg exchange couplings and single-ion anisotropies accounts for all the observed spin-wave dispersions and intensities. Along the b axis an unusually strong next-nearest-neighbor AF coupling competes with the dominant nearest-neighbor AF exchange interaction and causes the IC structure.

Strongly correlated systems with electronic and magnetic interactions have attracted much attention recently. Noted among them are the high-temperature superconductors, the colossal-magneto-resistance materials, and the multiferroics.[1] The latter group of materials possess magnetic and ferroelectric phases that may even coexist over a range of temperatures.[2] For some, the correlations are manifested in the magnetoelectric (ME) effect in which a magnetic field induces an electric polarization and an electric field induces a magnetic moment.[3] The lithium orthophosphates LiMPO$_4$, with M=Mn, Fe, Co, and Ni, constitute a prototypical isostructural group of antiferromagnets (AF) that are ME below their Néel temperatures.[4,5] Although they have been investigated for long,[4] a general consensus about the microscopic interactions leading to their ME effect has not yet been established.[6,7]

Here we focus on LiNiPO$_4$ which compared to its lithium orthophosphate (LO) counterparts has more complex magnetic ordering properties and a different temperature dependence of the linear ME coefficients.[4,8] LiNiPO$_4$ is orthorhombic with *Pnma* (no. 62) symmetry, lattice parameters $a=10.02$ Å, $b=5.86$ Å, $c=4.68$ Å, and 4 f.u./unit cell.[9] The magnetic Ni^{2+} ions with spin $S=1$ are located on the 4(c) sites and form buckled planes perpendicular to the crystallographic a axis. All LO compounds have low-temperature zero-field commensurate (C) AF phases, but only LiNiPO$_4$ passes via a first-order phase transition at $T_N=20.8$ K into an incommensurate (IC) AF phase with ordering temperature $T_{IC}=21.7$ K. Above T_{IC} short-range correlations persist up to 40 K.[8] In a recent study we have determined the magnetic structures and (H,T) phase diagram as function of temperature and magnetic field up to 14.7 T applied along the c axis.[7] Here we also suggested a microscopic model account-

ing for the symmetry and temperature dependence of the measured ME coefficients.[8] The present inelastic neutron scattering study is aimed at determining the magnetic couplings in LiNiPO$_4$ to improve our knowledge of the magnetic phases. Although the C phase has the general ordering vector $\mathbf{k}_C=(0,0,0)$ we find an anomalous shallow minimum in the magnon dispersion along the b direction at a modulation vector $\mathbf{q}_m\approx(0,0.12,0)$ (in reciprocal-lattice units). This is in the range of the IC ordering vector, $\mathbf{k}_{IC}=(0,q,0)$, where q is increasing with temperature between $0.07<q<0.155$.[8] Our analyses of the spin-wave spectra show that the minimum at $\mathbf{q}_m$ results from competing nearest-neighbor (NN) and next-nearest-neighbor (NNN) AF interactions along the b axis, and that the low-temperature zero field AF structure is on the verge between C and IC orders.

A high quality single crystal with approximate dimensions $5\times5\times9$ mm^3 and weight 0.4 g was used for this study. Inelastic neutron scattering measurements were performed on the RITA-II spectrometer (SINQ, PSI) by varying the incident energy at constant q to obtain dispersions along $(q,1,0)$ and $(0,1+q,0)$. RITA-II uses a seven-blade analyzer and a final energy of 5 meV.[10] Spin waves along the three principal directions, $(q,1,0)$, $(0,1+q,0)$, and $(0,1,q)$ were measured on the HB1A spectrometer (HFIR, Oak Ridge) with 14.7 meV initial energy and were within uncertainties the same as those measured on RITA-II. More than an entire Brillouin zone in the bc plane was also measured on the IN8 spectrometer (ILL), using a 47 channel multianalyzer-detector (Ref. 11) set for a final energy of 30 meV.

The spin-wave dispersions and integrated intensities measured at RITA-II and HB1A along the a-, b-, and c directions at low temperatures are shown in Fig. 1. The $(q,1,0)$ and
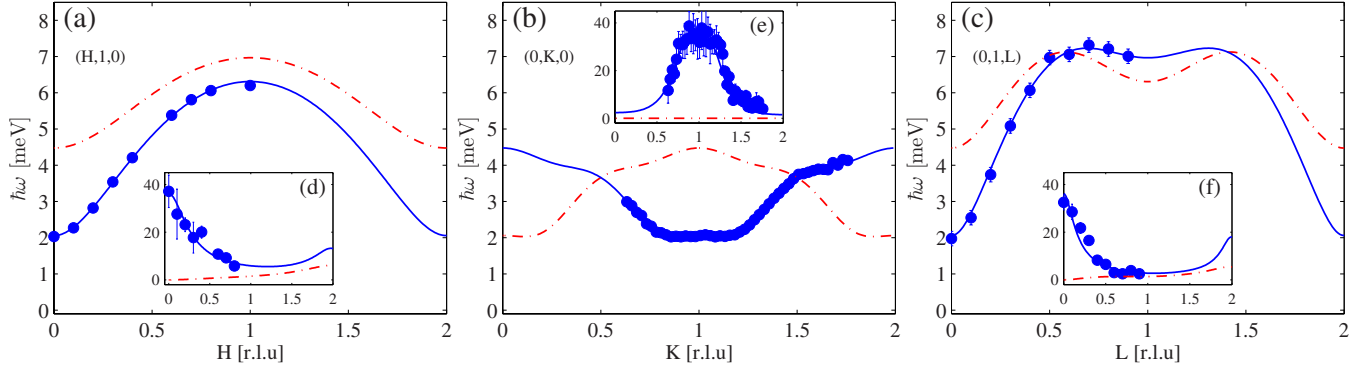
FIG. 1. (Color online) Measured (filled circles) spin-wave dispersion along three reciprocal directions, compared with a Holstein-Primakoff spin-wave calculation (full and dotted lines) as explained in the text. The insets show the corresponding measured and calculated intensities (in arbitrary units) as function of wave vector. The dispersions along $(H,1,0)$ and $(0,K,0)$ were measured at $T=2$ K on RITA-II, while the dispersion along $(0,1,L)$ was measured at $T=10$ K on HB1A.

$(0,1,q)$ dispersions behave as expected for an antiferromagnet with an energy gap at the zone center, but the dispersion along $(0,1+q,0)$ is unusual. It is almost a constant at low q with a shallow minimum at $q \approx 0.12$, corresponding to the observed IC ordering vectors just below T_{IC}.[8] Generally, the $(0,1+q,0)$ modes are lower in energy than along the two other principal directions, and they soften the same way as the $q=0$ mode when the temperature increases toward the C-IC transition temperature T_N. Figure 2 shows the temperature dependence of the spin-wave gap at $\mathbf{Q}=(0,1,0)$. The inset displays spin-wave neutron scattering spectra at $\mathbf{Q}=(0,1.055,0)$, close to the q value of the IC-modulation vector found just above T_N. No spin-waves were observed in the IC phase.

As a basis for our spin-wave model we adopt the AF ground state of the Ni^{2+} ions determined by Santoro *et al.*[12] and Vaknin *et al.*[13] with antiparallel spins pointing along the c axis as shown in Fig. 2(b). In fact, the spins are canted slightly away from the c axis,[7,14] consistent with a Dzyaloshinsky-Moria interaction, but this has negligible influence on the linear spin-wave model presented here. Ac-

cordingly, we use the following spin Hamiltonian for $LiNiPO_4$, with Heisenberg interactions J_{ij} and standard single-ion anisotropy terms $D_\alpha (S^\alpha)^2$ ($\alpha = a, b, c$):

$$\mathcal{H} = \sum_{i,j} J_{ij} \mathbf{S}_i \cdot \mathbf{S}_j + \sum_{i,\alpha} D_\alpha (S_i^\alpha)^2. \tag{1}$$

In the bc plane the Ni spins are coupled via superexchange Ni^{2+}-O-Ni^{2+} bonds, and our model includes NN interactions, J_{bc}, with a 3.81 Å bond length, and two NNN, J_b and J_c, with 4.71 and 5.89 Å bonds, respectively. For the couplings between the bc planes we consider NN interactions J_{ab} and J_{ac}, which have 5.40 and 5.50 Å bond lengths [see Fig. 2(b)]. The interplane couplings are mediated by PO_4-tetrahedra and may have a significant magnitude, e.g., as found in $Li_3Fe_2(PO_4)_3$.[15]

Using linear spin-wave theory we have calculated the spin-wave dispersions and intensities by a Holstein-Primakoff approach similar to the one described in Ref. 16. The two spin-wave dispersions derived from Eq. (1) are given by (for details see Ref. 14),

$$\hbar\omega = \sqrt{A^2 - (B \pm C)^2}, \tag{2}$$

where

$$\begin{aligned} A &\equiv 4S(J_{bc} + J_{ab}) - 2S\{J_b[1 - \cos(\mathbf{Q} \cdot \mathbf{r}_5)] \\ &\quad + J_c[1 - \cos(\mathbf{Q} \cdot \mathbf{r}_6)] + J_{ac}[2 - \cos(\mathbf{Q} \cdot \mathbf{r}_7) \\ &\quad - \cos(\mathbf{Q} \cdot \mathbf{r}_8)]\} + (S - 1/2)(D_a + D_b), \end{aligned}$$
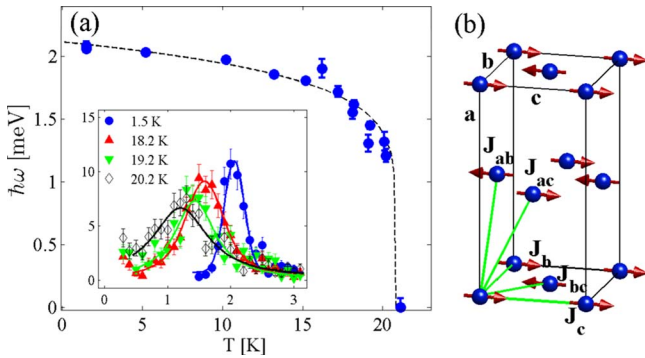
$$B \equiv (S - 1/2)(D_a - D_b),$$

FIG. 2. (Color online) (a) Spin-wave energy gap at $\mathbf{Q}=(0,1,0)$ as function of temperature measured at RITA-II. The dashed line is a guide to the eyes. The inset shows constant $\mathbf{Q}=(0,1.055,0)$ scans at different temperatures with $\hbar\omega$ (in meV) along the x axis and measured intensity (in counts per minute) along y. (b) The magnetic unit cell of $LiNiPO_4$ showing only Ni^{2+} ions. The depicted spin configuration and exchange interactions are the ones used in the spin-wave model.

TABLE I. The fitted spin coupling constants for $LiNiPO_4$. All units are in meV. By definition: $D_c \equiv 0$ meV.

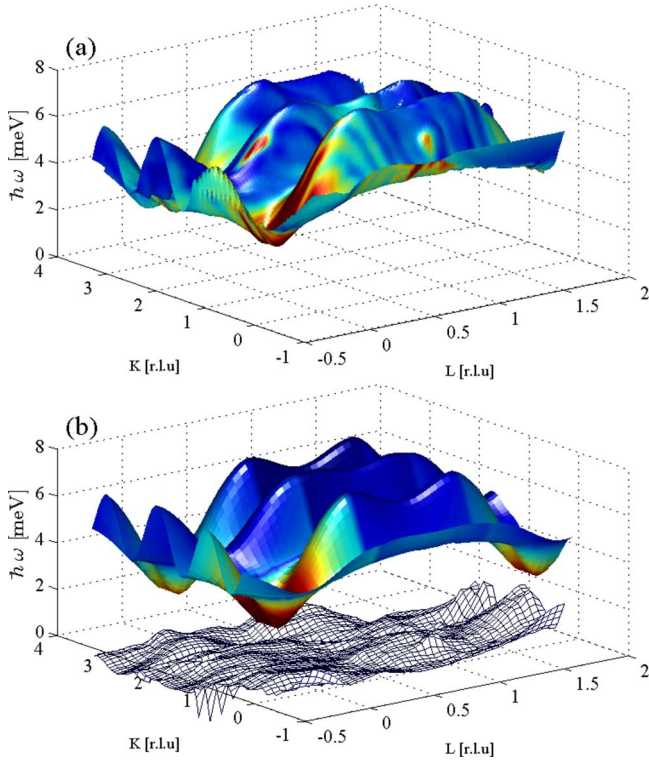| J_{bc}	J_b	J_c	J_{ab}	J_{ac}	D_a	D_b
1.04(6)	0.670(9)	−0.05(6)	0.30(6)	−0.11(3)	0.339(2)	1.82(3)

FIG. 3. (Color online) Spin-wave dispersions in the $(0, K, L)$ plane corresponding to the most intense branch. In colors we present spin-wave intensities with red for high and blue for low intensity. (a) Experimental data from IN8 at ILL. (b) Calculated data using the spin-wave model described in the text. The mesh around 0 meV shows the deviation in energy between (a) and (b).

$$C \equiv 2J_{bc}S[\cos(\mathbf{Q} \cdot \mathbf{r}_1) + \cos(\mathbf{Q} \cdot \mathbf{r}_2)] + 2J_{ab}S[\cos(\mathbf{Q} \cdot \mathbf{r}_3) + \cos(\mathbf{Q} \cdot \mathbf{r}_4)].$$

Here $\mathbf{r}_i$ denotes vectors between NN or NNN Ni ions, and

are: $\mathbf{r}_{1,2} = \frac{1}{2}(\mathbf{b} \pm \mathbf{c})$, $\mathbf{r}_{3,4} = \frac{1}{2}(\mathbf{a} \pm \mathbf{b})$, $\mathbf{r}_5 = \mathbf{b}$, $\mathbf{r}_6 = \mathbf{c}$, and $\mathbf{r}_{7,8} = \frac{1}{2}(\mathbf{a} \pm \mathbf{c})$.

The model parameters were determined by a simultaneous least-squares refinement of the spin-wave dispersions in all three principal directions.[17] The best fit is shown by full and dotted lines in Fig. 1, and the refined parameters are listed in Table I. The couplings J_{ac} and J_c assure ferromagnetically ordered ac planes that interact via $J_{bc}+J_{ab}$ to NN and J_b to NNN ac planes along the b direction. All interactions J_{bc}, J_{ab} (NN), and J_b (NNN) are AF which leads to frustration promoting the IC ordering. We note that the J_{ab} and J_{ac} couplings in the a direction are somewhat weaker than J_{bc} and J_b. This is consistent with the findings in Ref. 13 where magnetic short-range fluctuations extending into the paramagnetic regime and a critical exponent $\beta = 0.12$ of the C order parameter indicates a near-two-dimensional magnetic ordering of the bc planes. The single-ion anisotropies, D_a and D_b, are both positive indicating that a c axis magnetic moment is favored in the ground state, as observed experimentally. It should be noted that it is not possible from Eq. (2) to determine which of the two is larger, D_a or D_b. However, comparing the calculated intensities to the measured ones (insets of Fig. 1) establishes unequivocally that $D_a < D_b$, as given in Table I.

From the symmetry of the magnetic structure it can be shown that at least two nondegenerate dispersions are needed to account for the spin wave in the b direction.[14] In our model calculations the existence of two nondegenerate branches is a result of the different anisotropies along a, b, and c. However, at RITA-II and HB1A (Fig. 1) we observed only a single magnon dispersion, either because the second branch had too low intensity (see Fig. 1 insets), or because the two dispersions were indistinguishable within instrumental resolution at the measured $\mathbf{Q}$ values. Searching for the second branch and further confirmation of our model, we used the IN8 spectrometer to collect data from a larger range of $\mathbf{Q}$ values in the bc plane. In Fig. 3 we compare a three-dimensional color map of the most intense spin-wave dispersion measured at IN8 (a) to the results of our model calcu-
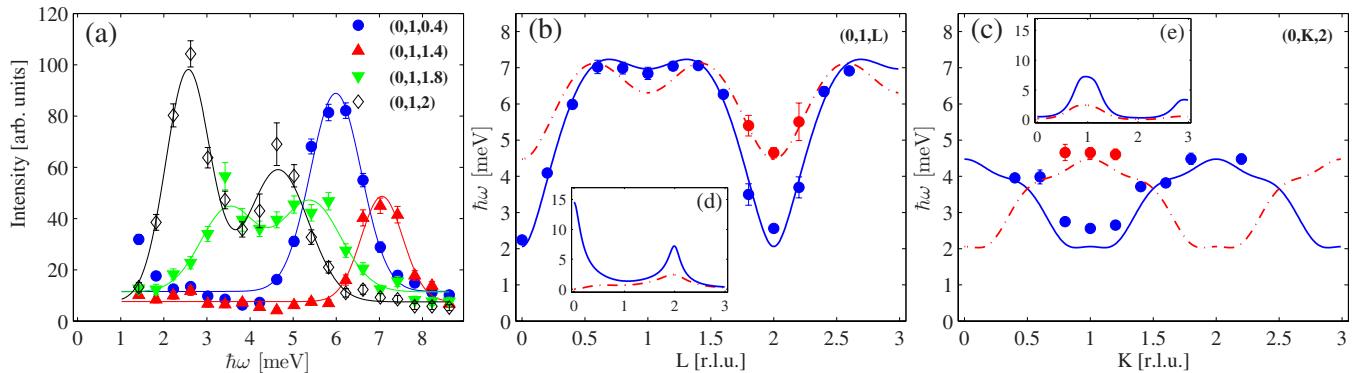

FIG. 4. (Color online) (a) Constant $\mathbf{Q}=(0,1,L)$ cuts from IN8. At $\mathbf{Q}=(0,1,0.4)$ and $(0,1,1.4)$ only a single branch is visible, but at $\mathbf{Q}=(0,1,1.8)$ and $(0,1,2)$ both branches are observed. (b) Dispersions along $(0,1,L)$ measured at IN8 [blue (black) and red (gray) circles compared to the calculated spin-wave energies (full and dotted lines). The inset shows the calculated intensity of the dispersions. Two branches are observed at $\mathbf{Q}$ where the model predicts spin-waves with finite intensity that are well separated in energy. (c) Dispersions along $(0,K,2)$ measured at IN8 and compared to the calculated spin-wave energies. The inset shows the calculated intensity of the branches. Along $(0,K,0)$ [Fig. 1(b)] the intensity of the second branch is always zero, but here, along $(0,K,2)$, there are $\mathbf{Q}$-values where both branches have intensity and can be observed.

lation (b) using the interaction parameters of Table I. The experiment at IN8 gave clear evidence of two nondegenerate magnon branches, as seen in Fig. 4. Here two-peak line-shapes were observed in energy scans at scattering vectors where the calculations predicted that the branches were well separated in energy and both had finite intensity.

The exchange interactions established in this work may be used to explain the magnetic ground state. Maximizing $J(\mathbf{Q}) = \Sigma J_{ij} e^{-i\mathbf{Q} \cdot \mathbf{R}_{ij}}$ at zero temperature shows that the IC order is favorable in a simple model of layered magnetic systems with competing interactions if the effective exchange interactions, J_1 and $J_2 > 0$, between NN and NNN ferromagnetic layers fulfill that $|J_1| < 4J_2$.[18] If this condition applies, the magnetic ordering vector Q is determined by $\cos(Qd) = -J_1/4J_2$, where d is the interlayer distance between adjacent ferromagnetic layers. Since $LiNiPO_4$ has ferromagnetic layers perpendicular to the b direction, we can test this condition. Here $J_1 = 2J_{bc} + 2J_{ab}$ and $J_2 = J_b$, while $d = b/2$. Using the exchange parameters in Table I we find: $J_1 = 2.7(2)$ meV and $4J_2 = 2.68(4)$ meV, for the competing interactions. Within

the uncertainties the magnetic ground state could therefore be either C or IC, and the system is close to an instability. A mean-field model using interaction parameters obtained from the spin-wave spectra predicts a behavior qualitatively similar to that observed experimentally.[19] Here it is found that the magnetic structure is IC just below T_{IC}, but that the extra lock-in anisotropy energy gained by the C structure becomes important at slightly lower temperatures and as result changes q from $\mathbf{k}_{IC}$ to 0.

[1] S.-W. Cheong and M. Mostovoy, Nature Mater. **6**, 13 (2007).

[2] M. Kenzelmann, A. B. Harris, S. Jonas, C. Broholm, J. Schefer, S. B. Kim, C. L. Zhang, S. W. Cheong, O. P. Vajk, and J. W. Lynn, Phys. Rev. Lett. **95**, 087206 (2005).

[3] W. Eerenstein, N. D. Mathur, and J. F. Scott, Nature (London) **442**, 759 (2006).

[4] M. Mercier, Ph.D. thesis, Université de Grenoble, 1969.

[5] J.-P. Rivera, Ferroelectrics **161**, 275 (1993).

[6] B. B. van-Aken *et al.*, Nature (London) **449**, 702 (2007).

[7] T. B. S. Jensen *et al.*, preceding paper, Phys. Rev. B **79**, 092412 (2009).

[8] D. Vaknin, J. L. Zarestky, J. P. Rivera, and H. Schmid, Phys. Rev. Lett. **92**, 207201 (2004).

[9] I. Abrahams and K. S. Easson, Acta Crystallogr., Sect. C: Cryst. Struct. Commun. **49**, 925 (1993).

[10] C. R. H. Bahl *et al.*, Nucl. Instrum. Methods Phys. Res. B **246**, 452 (2006).

[11] F. Demmel, N. Grach, and H. M. Rønnow, Nucl. Instrum. Methods Phys. Res. A **530**, 404 (2004).

[12] R. P. Santoro, D. J. Segal, and R. E. Newnham, J. Phys. Chem. Solids **27**, 1192 (1966); R. P. Santoro and R. E. Newnham, Acta Crystallogr. **22**, 344 (1967).

[13] D. Vaknin, J. L. Zarestky, J. E. Ostenson, B. C. Chakoumakos, A. Goni, P. Pagliuso, T. Rojo, and G. E. Barberis, Phys. Rev. B **60**, 1100 (1999).

[14] T. B. S. Jensen, Ph. D. thesis, Risø DTU and University of Copenhagen, 2007, www.bricksite.com/tstibius.

[15] J. L. Zarestky *et al.*, J. Magn. Magn. Mater. **234**, 401 (2001).

[16] P. A. Lindgård, A. Kowalska, and P. Laut, J. Phys. Chem. Solids **28**, 1357 (1967).

[17] Since the energy gap does not change significantly between 2 and 10 K we used the same interaction parameters when fitting at 2 and 10 K.

[18] T. Nagamiya, in *Solid State Physics*, edited by F. Seitz and D. Turnbull (Academic, New York, 1967), Vol. 29, p. 346.

[19] J. Jensen (private communication).